Langmuir Article

pubs.acs.org/Langmuir

On the Thermodynamic Stability of α,ω-Alkanedithiols Self-Assembled Monolayers on Unreconstructed and Reconstructed Au(111)

P. Carro,*,† A. Hernandez Creus,† A. Muñoz,‡ and R. C. Salvarezza§

†Departamento de Química Física, and ‡Departamento de Física Fundamental II and MALTA Consolider Team, Universidad de La Laguna, Tenerife, Spain, and §Instituto de Investigaciones Fisicoquímicas Teóricas y Aplicadas (INIFTA), 1900 La Plata, Buenos Aires, Argentina

Received January 13, 2010. Revised Manuscript Received April 4, 2010

A comparative study on the thermodynamic stability of the lying down (**LD**) and standing up (**SU**) phases of α,ω-butanedithiol (BDT) on unreconstructed (U) and on reconstructed (R) Au(111) surfaces is presented. The R surface is made of dithiol-Au adatom units. Density functional calculations (DFT) allow the estimation of the adsorption energy of the **LD** and **SU** BDT phases on both substrates. Surface free energies based on the DFT calculations show the coverage of the clean Au(111) surface by the **LD** phase, and the **LD** to **SU** phase transition as the chemical potential of the BDT molecule is increased. The **LD** and **SU** phases are more stable on R than on U substrates, suggesting that the Au(111) surface should reconstruct upon BDT adsorption. The stability analysis is extended to longer α,ω-dithiols. Results reveal that the **LD** to **SU** phase transition is favored as the hydrocarbon chain length of the dithiol molecule is increased. Changes in the hydrogen pressure affect the formation of the **LD** phase, while they have only minor effects on the **LD** to **SU** phase transitions. Our calculations explain the influence of the number of carbon atoms in the hydrocarbon chains, hydrogen pressure and dithiol pressure (or concentration) on dithiol adsorption, and phase transitions. This information is relevant to control the coverage, reactivity, and surface chemistry of the α,ω-dithiol self-assembled monolayers on Au surfaces.

1. Introduction

Self-assembled monolayers (SAMs) of dithiols have attracted considerable interest because of the possibility of using them as linkers between two metallic centers such as nanoparticles, metallic surfaces, or thin films or to form nanocontacts using scanning tunneling microscopy tips.[1−5] In fact, the presence of two reactive functional SH groups allow these molecules to be exceptional linkers for a variety of metals. Several works on the preparation and application of dithiol SAMs are available in the literature.[1,6] However, the experimental conditions for the formation of well-ordered SAMs with free SH end-groups have been the object of much controversy.[7−9] One of the problems is related to the formation of the initial lying-down (**LD**) phase with the two -SH groups of the molecule bonded to the surface. The additional S−Au bond stabilizes the **LD** phase and thus increases the activation energy for conformational transformation to a standing-up (**SU**) phase.[8] In this way, the **LD** to **SU** phase transition could be completely inhibited by kinetics traps. However, the formation of **LD**, mixed (**LD** + **SU**), and **SU** phases depending on the chain length and self-assembly conditions has been reported.[8−10]

In this context, short dithiols are particularly interesting as a starting point, because in most cases, only the **LD** phase has been observed in a wide range of experimental conditions. Recent experimental data on these systems have shown that α,ω-butanedithiol[10] and dithiothreitol (DTT),[11] a four carbon α,ω-dithiol with hydroxyl groups on the second and third carbons, are self-assembled on Au(111) only in the **LD** configuration irrespective of the concentration and temperature. XPS and electrochemical data for these SAMs are consistent with a dithiol surface coverage of $\theta = 0.16$, with two S-head−Au covalent bonds per dithiol molecule. The surface coverage observed for BDT and DTT has been described in terms of $2\sqrt{3}\times\sqrt{3}\ R30°$ lattice.[12] On the other hand, for α,ω-hexanedithiol (HDT) experimental results are contradictory, as **LD**[8] or mixed domain (**LD** + **SU**)[10] phases have been reported. In fact, it has been proposed that the formation of a dense layer of dithiol molecules in **LD** configuration is able to trap the system in a metastable state.[8] In contrast, STM[13] and XPS[10] data for α,ω-nonanedithiol (NDT) have shown domains of $\sqrt{3}\times\sqrt{3}\ R30°$ thiolate lattice and SAM surface coverage of $\sim\theta = 0.33$, i.e., with most of the dithiol molecules in the **SU** arrangement. From the above discussion, it is evident that a careful investigation of the factor that induces the **LD** to **SU** phase transition is needed.

*Corresponding author. E-mail: pcarro@ull.es. Fax: 922 31 80 33.

(1) Liang, J.; Rosa, L. G.; Scoles, G. *J. Phys. Chem. C* **2007**, *111*, 17275–17284.
(2) Sakotsubo, Y.; Ohgi, T.; Fujita, D.; Ootuka, Y. *Appl. Surf. Sci.* **2005**, *241*, 33–37.
(3) Wierzbinski, E.; Slowinski, K. *Langmuir* **2006**, *22*, 5205–5208.
(4) Haiss, W.; Nichols, R. J.; Higgins, S. J.; Bethell, D.; Hobenreich, H.; Schiffrin, D. J. *Faraday Discuss.* **2004**, *125*, 179–194.
(5) Cui, X. D.; Primak, A; Zarate, X.; Tomfohr, J.; Sankey, O. F.; Moore, A. L.; Moore, T. A.; Gust, D.; Harris, G.; Lindsay, S. M. *Science* **2001**, *294*, 571–574.
(6) Henderson, J. I.; Feng, S.; Ferrence, G. M.; Bein, T.; Kubiak, C. P. *Inorg. Chim. Acta* **1996**, *242*, 115–124.
(7) Kohli, P.; Taylor, K. K.; Harris, J. J.; Blanchard, G. J. *J. Am. Chem. Soc.* **1998**, *120*, 11962–11968.
(8) Leung, T. Y. B.; Gerstenberg, M. C.; Lavrich, D. J.; Scoles, G.; Schreiber, F.; Poirier, G. E. *Langmuir* **2000**, *16*, 549–561.
(9) Hamoudi, H.; Guo, Z.; Prato, M.; Dablemont, C.; Zheng, W. Q.; Bourguignon, B.; Canepa, M.; Esaulov, V. A. *Phys. Chem. Chem. Phys.* **2008**, *10*, 6836–6841.
(10) Daza Millone, M. A.; Hamoudi, H.; Rodriguez, L.; Rubert, A.; Benitez, G.; Vela, M. E.; Salvarezza, R. C.; Gayone, J.; Sanchez, E.; Grizzi, O.; Dablemont, C.; Esaulov, V. *Langmuir* **2009**, *25*, 12945–12953.
(11) Creczynski-Pasa, T. B.; Daza Millone, M. A.; Munford, M. L.; de Lima, V. R.; Vieira, T. O.; Benitez, G. A.; Pasa, A. A.; Salvarezza, R. C.; Vela, M. E. *Phys. Chem. Chem. Phys.* **2009**, *11*, 1077–1084.
(12) MacDairmid, A. R.; Gallagher, M. C.; Banks, J. T. *J. Phys.Chem. B* **2003**, *107*, 9789–9792.
(13) Terán Arce, F.; Vela, M. E.; Salvarezza, R. C.; Arvia, A. J. *Surf. Rev. Lett.* **1997**, *4*, 637–649.

Another problem is that the Au−S interface for dithiols has not been explored in light of the recent adatom models proposed for the alkanethiol SAMs on Au(111) that have originated a strong debate in the scientific community.[14] The Au(111) surface reconstruction upon dithiol adsorption is supported by STM images where the typical vacancy Au islands are resolved.[11,12]

In this work, we investigate the thermodynamic stability of the lying-down (**LD**) and standing-up (**SU**) phases of butanedithiol (BDT) either on an unreconstructed Au(111) (U) or on reconstructed Au(111) (R) made of dithiol-Au adatom units. These species have been considered to be present in diluted[15] and dense phases of alkanethiols on Au(111) .[14,16] Surface free energies based on the DFT data show the initial adsorption of the BDT molecules on the clean Au(111) surface forming the **LD** phase followed by the **LD** to **SU** phase transition as the chemical potential of the BDT molecule is increased. The **LD** and **SU** phases are more stable on the R than on U substrates, suggesting that the Au(111) surface should reconstruct upon BDT adsorption. Phase diagrams for HDT and NDT show that the **LD** to **SU** phase transitions are favored by increasing the hydrocarbon chain length of the dithiol molecules, thus explaining the experimental data reported for this system. The parameters that control the thermodynamic stability of the different phases are the binding energy of the adsorbates and the number of adsorbed species per unit of substrate area.

2. Methodology

All calculations were performed using plane-wave pseudopotential periodic DFT. The exchange-correlation potential was described by means of the generalized gradient approach (GGA) with the Perdew−Wang (PW91)[17] implementation. The one-electron wave functions have been expanded on a plane wave basis set with a cutoff of 420 eV for the kinetic energy. The Brillouin zone sampling is carried out according to the Monkhorst-Pack[18] scheme with $(5 \times 5 \times 1)$ dense k-point meshes. The projector augmented wave (PAW) method[19,20] as implemented by Kresse and Joubert[21] has been employed to describe the effect of the inner cores of the atoms on the valence electrons. The tolerance used to define self-consistency is 10^{-5} eV for the single-point total energy and 10^{-4} eV for the geometry optimization. The energy minimization (electronic density relaxation) for a given nuclear configuration is carried out using a Davidson block iteration scheme. The dipole correction is applied to minimize polarization effects caused by asymmetry of the slabs. All calculations have been carried out using the *VASP 4.6* package.[21,22]

The surface is modeled by a periodic slab composed of five metal layers and a vacuum of ∼12 Å. Adsorption occurs only on one side of the slab. During the geometry optimization, the two bottom layers were kept fixed at their optimized bulk truncated geometry for the Au(111) surface. The three outermost atomic metal layers as well as the atomic coordinates of the adsorbed species were allowed to relax without further constraints. The atomic positions were relaxed until the force on the unconstrained atoms was less than 0.03 eV/ Å. The unit cell employed in all calculations was a $(3 \times 2\sqrt{3})$ of the Au(111) surface that contains two BDT in **LD** phase or four BDT in **SU** one. In the reconstructed surface study, the unit cell contains two Au adatoms. The molecular calculations of BDT, **LD**, **SU**, and H_2 are done in a cubic supercell with side lengths of $(20 \times 20 \times 20)$ Å. The lattice parameter calculated for Au bulk is 4.18 Å.

The average binding energy per species adsorbed on Au(111) surface is defined as in eq 1

$$E_b^{X/Au} = \frac{1}{N_X}\left[E^{X/Au} - E^{Au} - N_X E_X\right] \quad (1)$$

where N_X ($N_{\mathbf{LD}}$ or $N_{\mathbf{SU}}$) is the number of adsorbed species in the surface unit cell for **LD** or **SU** phases, respectively. $E^{X/Au}$, E^{Au}, and E_X ($E_{\mathbf{LD}}$ or $E_{\mathbf{SU}}$) stand for the total energy of the (**LD** or **SU**)-substrate system, for the clean surface, and the energy of the adsorbed diradical or radical (**LD**, **SU**), respectively. Negative numbers indicate an exothermic adsorption process with respect to the clean surface and the adsorbed X phases originated during the adsorption process from the BDT molecule.

The optimized structures for **LD** and **SU** phases on the U substrate are presented in Figure 1. The **SU** phases consist of the well-known $\sqrt{3}\times\sqrt{3}$ $R30°$ (Figure 1b) and $c(4 \times 2)$ (Figure 1c) lattices with surface coverage $\theta = 1/3$, both extensively described for alkanethiolates SAMs on the same substrate.[23] In the **LD** phase (Figure 1a), the alkyl chains are not fully extended (looped). In fact, while the S−S intramolecular distance in the BDT isolated molecule is 0.68 nm on the Au surface the BDT molecule must adopt the ∼0.5 nm nearest-neighbor distance needed to fit the coverage $\theta = 1/6$ experimentally observed.[12] The optimized configurations show that S atoms are bonded to the Au(111) surface at hollow fcc-bridge positions for both the **LD** and $\sqrt{3}\times\sqrt{3}$ $R30°$ **SU** phases. On the other hand, the $c(4 \times 2)$ **SU** phase exhibits 1/2 S atoms at hollow fcc-bridge sites and 1/2 S atoms at hollow hcp-bridge sites. In the **SU** phase, the tilt angle, the angle between the molecular backbone and the surface normal direction, is ∼40°, close to those reported for these systems.[24,25]

In the reconstructed Au(111) surface, the **LD** and **SU** phases involve thiolate-Au adatom species (Figure 2). The Au adatoms are placed in the bridge site of the substrate. In **LD** phase, the BDT molecule is placed parallel to the surface with both S atoms at the same level above the surface as the Au adatom. Each BDT molecule is placed between two different Au adatoms forming a polymeric chain (Figure 2a). This leads to one thiolate per Au adatom relationship. Also in this case, the alkyl chains are not fully extended because the molecule must reach a ∼0.5 nm nearest-neighbor distance between the Au adatoms to satisfy $\theta = 1/6$ experimentally observed.[12] In the case of the **SU** phase, the lattice consists of two BDT-Au-BDT units in a $3\times2\sqrt{3}$ unit cell, i.e., the $c(4 \times 2)$ surface structure with $\theta = 1/3$ (Figure 2b). Only one of the two S atoms of the BDT molecule is bonded to the Au adatom.

Also in this case, the tilt angle between the hydrocarbon chain and the surface normal is ∼40°. As already noted for alkanethiols,

(14) Woodruff, D. P. *Phys. Chem. Chem. Phys.* **2008**, *10*, 7211–7221.
(15) Maksymovych, P.; Sorescu, D. C.; Yates, J. J. T. *Phys. Rev. Lett.* **2006**, *97*, 146103–146104.
(16) Walter, M.; Akola, J.; Lopez-Acevedo, O.; Jadzinsky, P. D.; Calero, G.; Ackerson, C. J.; Whetten, R. L.; Grönbeck, H.; Häkkinen, H. *Proc. Natl. Acad. Sci. U.S.A.* **2008**, *105*, 9157–9162.
(17) Perdew, J. P.; Chevary, J. A.; Vosko, S. H.; Jackson, K. A.; Pederson, M. R.; Singh, D. J.; Fiolhais, C. *Phys. Rev. B* **1991**, *46*, 6671–6687.
(18) Monkhorst, H. J.; Pack, J. D. *Phys. Rev. B* **1976**, *13*, 5188–5192.
(19) Blöchl, P. E. *Phys. Rev. B* **1994**, *50*, 17953–17979.
(20) Blöchl, P. E.; Marga, P.; Schwarz, K. Ab initio molecular dynamics with the projector augmented wave method. In *Chemical Application of Density-Functional Theory*; American Chemical Society: Washington, DC, 1996.
(21) Kresse, G.; Joubert, D. *Phys. Rev. B* **1998**, *59*, 1758–1775.
(22) Kresse, G.; Furthmüller *J. Phys. Rev. B* **1996**, *54*, 11169–11185.
(23) Vericat, C.; Vela, M. E.; Benitez, G. A.; Martin Gago, J. A.; Torrelles, X.; Salvarezza, R. C. *J. Phys: Condens. Matter* **2006**, *18*, R867–R900.
(24) Porter, M. D.; Bright, T. B.; Allara, D. L.; Chidsey, C. E. D. *J. Am. Chem. Soc.* **1987**, *109*, 3559–3568.
(25) Snyder, R. G.; Maroncelli, M.; Strauss, H. L.; Hallmark, V. M. *J. Phys. Chem.* **1986**, *90*, 5623–5630.

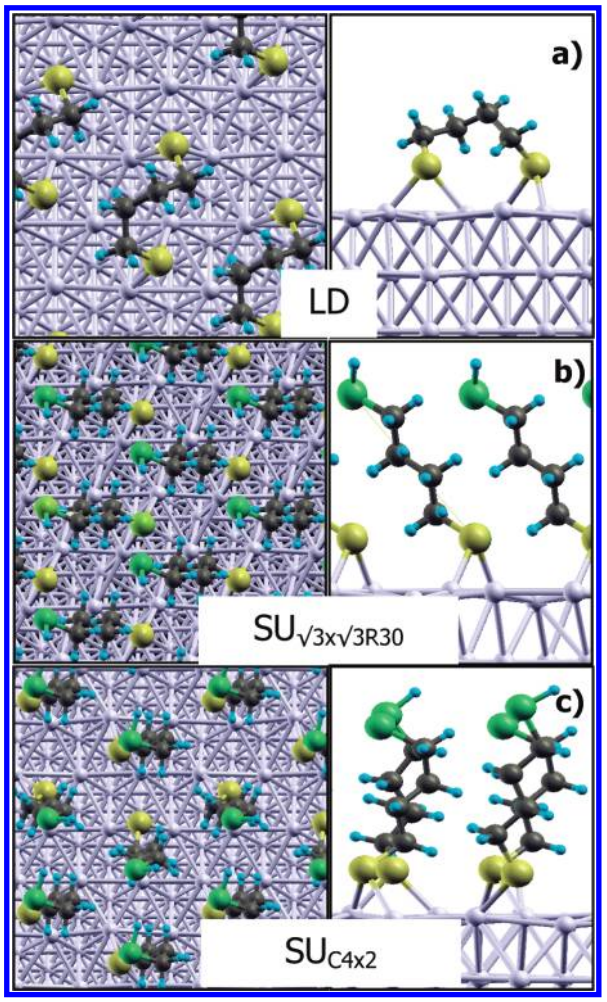

Figure 1. Equilibrium structures of BDT adsorbed on unreconstructed (U) Au(111) for (a) lying-down (**LD**) and (b,c) standing-up (**SU**) phases in (b) $\sqrt{3}\times\sqrt{3}$ $R30°$ lattice and (c) $c(4 \times 2)$ lattice. Left: Top view. Right: Side view. White, Au; yellow: S (bonded to gold); brown, C; green, S (HS group); light blue, H.

the BDT-Au-BDT units with $\theta = 1/3$ are only compatible with the $c(4 \times 2)$ surface structure.[26] Note that a model involving one alkanethiol on top of one Au adatom, which is consistent with the $\sqrt{3} \times \sqrt{3}$ $R30°$ lattice, is unstable even with respect $\sqrt{3}\times\sqrt{3}$ $R30°$ on the unreconstructed Au(111) surface.[28]

While other surface structure models, in particular, more diluted **LD** phases, have been described for dithiols, in this paper we have restricted our analysis to the five surface structures described in Figures 1 and 2.

Thermodynamic Stability of the LD and SU Phases. The formation of the **LD** and **SU** phases when BDT molecules from the gas phase are placed in contact with the clean Au(111) surface can be described by the following reactions:

$$\mathrm{BDT} + \mathrm{Au(111)} \rightarrow \mathrm{BDT_{LD}/Au(111)} + \mathrm{H_2} \qquad (2)$$

$$2\mathrm{BDT} + \mathrm{Au(111)} \rightarrow 2\mathrm{BDT_{SU}/Au(111)} + \mathrm{H_2} \qquad (3)$$

In eq 2, one BDT molecule reacts with the Au(111) surface forming an adsorbed BDT species in **LD** configuration (with two thiolate-Au bonds) and one hydrogen molecule produced by the cleavage of the two S−H bonds of the BDT molecule. Similarly, in eq 3 two BDT molecules react with the Au(111) surface forming two adsorbed BDT species in **SU** configuration (with one thiolate-Au bond per molecule) and one hydrogen molecule produced by the cleavage of the S−H bonds.

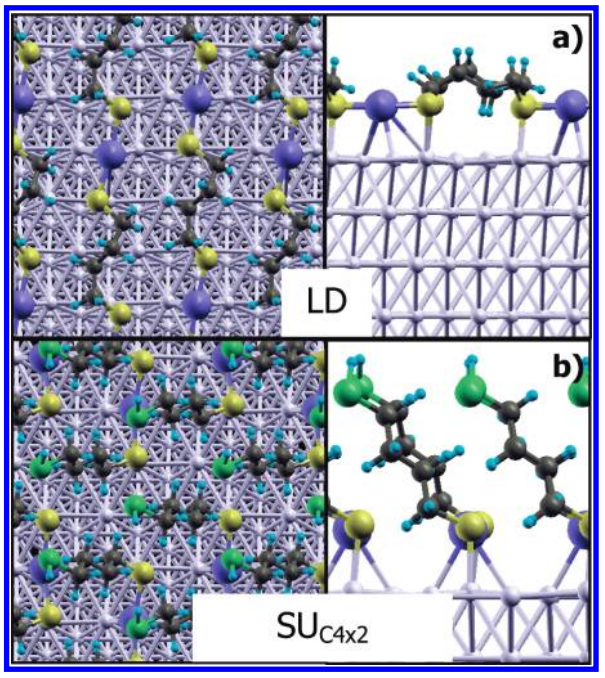

Figure 2. Equilibrium structures of BDT adsorbed on reconstructed (R) Au(111) for (a) lying-down (**LD**) and (b) standing-up (**SU**) phases in $c(4 \times 2)$ lattice. Left: Top view. Right: Side view. White, Au; lyle, Au adatom; yellow, S (bonded to Au); brown, C; green, S (HS group); light blue, H.

Following our previous work,[27,28] in order to compare the stability of the these phases containing different surface arrangements, different numbers of S−Au bonds, and different numbers of adsorbed species, we make use of the surface free energy,[29] defined by

$$\gamma = \frac{1}{A}\left[G^{X/\mathrm{Au}} - N_{\mathrm{Au}}\mu_{\mathrm{Au}} - N_X\mu_X\right] - \gamma_{\mathrm{clean}} \qquad (4)$$

where A is the surface area, $G^{X/\mathrm{Au}}$ is the Gibbs free energy of the adsorbed system, and μ_{Au} and μ_X are the chemical potentials of the bulk metal surface and the adsorbate, respectively. N_{Au} and N_X are the number of gold atoms and the adsorbed species in the slab unit cell. On the other hand, γ_{clean} represents the surface free energy of the clean surface.

In eq 4, the chemical potential of the Au surface (μ_{Au}) is equated to the total energy of a bulk Au atom ($E^{\mathrm{Au}}_{\mathrm{Bulk}}$). On the other hand, the Gibbs free energy ($G^{X/\mathrm{Au}}$) is estimated by the total energy of the adsorbate−substrate system at $T=0$ K ($E^{X/\mathrm{Au}}$) plus the vibrational contribution to the Gibbs free energy (F_{vib}) that involves both the vibrational energy and entropy, as shown in eq 5.

$$G^{X/\mathrm{Au}} = E^{X/\mathrm{Au}} + F_{\mathrm{vib}} \qquad (5)$$

In the case of F_{vib}, only vibrations of the adsorbed species are considered. The contribution of Au atoms is neglected since their vibrational contributions in the clean and the adsorbed system are canceled.

(26) Voznyy, O.; Dubowski, J. J. *Langmuir* **2009**, *25*, 7353–7358.
(27) Torres, D.; Carro, P.; Salvarezza, R. C.; Illas, F. *Phys. Rev. Lett.* **2006**, *97* (226103), 1–4.
(28) Carro, P.; Salvarezza, R. C.; Torres, D.; Illas, F. *J. Phys. Chem. C* **2008**, *112*, 19121–19124.
(29) Reuter, K.; Scheffler, M. *Phys. Rev. B* **2002**, *65*(035406), 1–11.

In reactions 2 and 3, the gas phase acts as a reservoir interchanging BDT and H_2 molecules with the surface. In principle, this picture could also be considered valid for BDT molecules in hexane where no dissociation of the SH groups takes place. Thus, the chemical potentials of the **LD** and **SU** phases can be written as a function of these species

$$\mu_{\mathbf{LD}} = \mu_{\mathrm{BDT}} - \mu_{\mathrm{H_2}} \tag{6}$$

$$\mu_{\mathbf{SU}} = \mu_{\mathrm{BDT}} - \frac{1}{2}\mu_{\mathrm{H_2}} \tag{7}$$

Now, we can define the chemical potential of the BDT molecules in relation to the DFT total energy (E_{BDT}), and the zero-point energy correction ($E^{\mathrm{ZPE}}_{\mathrm{BDT}}$) as follows

$$\mu_{\mathrm{BDT}} = E_{\mathrm{BDT}} + E^{\mathrm{ZPE}}_{\mathrm{BDT}} + \Delta\mu_{\mathrm{BDT}} \tag{8}$$

where

$$\Delta\mu_{\mathrm{BDT}} = \mu^0_{\mathrm{BDT}}(T, p^0) + k_{\mathrm{B}}T\ln\left(\frac{p_{\mathrm{BDT}}}{p^0}\right) \tag{9}$$

Equation 9 includes p and T implicitly considering ideal gas behavior. $\mu^0_{BDT}(T, p^0)$ is the chemical potential relative to the standard-state pressure, p^0, which has been estimated in terms of the molecular partition function as shown in the Supporting Information. In order to calculate the chemical potential of the hydrogen molecule, we have used eq 10

$$\mu_{\mathrm{H_2}}(T,p) = E_{\mathrm{H_2}} + E^{\mathrm{ZPE}}_{\mathrm{H_2}} + \mu^0_{\mathrm{H_2}}(T,p^0) + k_{\mathrm{B}}T\ln\left(\frac{p_{\mathrm{H_2}}}{p^0}\right) \tag{10}$$

where k_{B} is the Boltzmann constant. The total energy $E_{\mathrm{H_2}}$and the zero-point energy correction $E^{\mathrm{ZPE}}_{\mathrm{H_2}}$ are estimated by DFT, and $\mu^0_{\mathrm{H_2}}$ can be taken from standard thermochemical tables.[30] We have used in our calculations $T = 300\ K$ and two partial hydrogen pressures $p_{\mathrm{H_2}} = 10^{-10}$ atm and $p_{\mathrm{H_2}} = 5 \times 10^{-7}$ atm. These values are reasonable, taking into account the amount of H_2 produced by reactions 2 and 3 in a UHV system, and the H_2 levels in a recipient containing hexane in contact with air (5×10^{-7} atm).

The most stable surface structure is the one which minimizes the surface free energy. The surface free energy as a function of the binding energy (eq 1) is given by

$$\gamma_{\mathbf{LD}}(\Delta\mu_{\mathrm{BDT}}) = \frac{N_{\mathbf{LD}}}{A}\left[E^{\mathbf{LD}/\mathrm{Au}}_{\mathrm{b}} - \left(E_{\mathrm{BDT}} - E_{\mathbf{LD}} - \mu_{\mathrm{H_2}} + E^{\mathrm{ZPE}}_{\mathrm{BDT}} - F^{\mathbf{LD}/\mathrm{Au}}_{\mathrm{vib}}\right)\right] + \gamma_{\mathrm{clean}} - \frac{N_{\mathbf{LD}}}{A}\Delta\mu_{\mathrm{BDT}} \tag{11}$$

$$\gamma_{\mathbf{SU}}(\Delta\mu_{\mathrm{BDT}}) = \frac{N_{\mathbf{SU}}}{A}\left[E^{\mathbf{SU}/\mathrm{Au}}_{\mathrm{b}} - \left(E_{\mathrm{BDT}} - E_{\mathbf{SU}} - \frac{1}{2}\mu_{\mathrm{H_2}} + E^{\mathrm{ZPE}}_{\mathrm{BDT}} - F^{\mathbf{SU}/\mathrm{Au}}_{\mathrm{vib}}\right)\right] + \gamma_{\mathrm{clean}} - \frac{N_{\mathbf{SU}}}{A}\Delta\mu_{\mathrm{BDT}} \tag{12}$$

with the surface free energy of the clean cell given by

$$\gamma_{\mathrm{clean}} = \frac{1}{A}\left[E^{\mathrm{Au}} - N_{\mathrm{Au}}E^{\mathrm{Au}}_{\mathrm{bulk}}\right] - \gamma^{\mathrm{U}}_{\mathrm{clean}} \tag{13}$$

In eq 13, $\gamma^{\mathrm{U}}_{\mathrm{clean}}$ is the surface free energy of the unreconstructed Au(111) surface, which has to be subtracted because the slab model exhibits two surfaces, one unreconstructed and without adsorbate and another one with adsorbate and reconstructed or not, depending on the case. Note that in the eqs 11 and 12 $N_{\mathbf{SU}} = 2N_{\mathbf{LD}}$.

It is well-known that the PW91 functional does not estimate the dispersion forces that should be not negligible in these systems. A reasonable estimation of these forces acting at the **LD** phase can be done by considering experimental data for alkane physisorbed on Au.[31] These data indicate that for each CH_2 the chain−substrate and chain−chain interactions increase 0.064 eV. Thus, we corrected the E_{b} values derived from our DFT calculations by adding $E_{\mathrm{vdW}} = -(n_{\mathrm{C}}\ 0.064\ \mathrm{eV})$, with n_{C} being the number of methylene units. For the **SU** phases, the chain/chain interaction should increase as $E_{\mathrm{vdW}} = -(n_{\mathrm{C}}\ 0.044\ \mathrm{eV})$.[32] Including E_{vdW} into eqs 11 and 12, one can obtain for the **LD** and **SU** phases

$$\gamma_{\mathbf{LD}}(\Delta\mu_{\mathrm{BDT}}) = \frac{N_{\mathbf{LD}}}{A}\left[\left(E^{\mathbf{LD}/\mathrm{Au}}_{\mathrm{b}} - n_{\mathrm{C}}0.064\right) - \left(E_{\mathrm{BDT}} - E_{\mathbf{LD}} - \mu_{\mathrm{H_2}} + E^{\mathrm{ZPE}}_{\mathrm{BDT}} - F^{\mathbf{LD}/\mathrm{Au}}_{\mathrm{vib}}\right)\right] + \gamma_{\mathrm{clean}} - \frac{N_{\mathbf{LD}}}{A}\Delta\mu_{\mathrm{BDT}} \tag{14}$$

$$\gamma_{\mathbf{SU}}(\Delta\mu_{\mathrm{BDT}}) = \frac{N_{\mathbf{SU}}}{A}\left[\left(E^{\mathbf{SU}/\mathrm{Au}}_{\mathrm{b}} - n_{\mathrm{C}}0.044\right) - \left(E_{\mathrm{BDT}} - E_{\mathbf{SU}} - \frac{1}{2}\mu_{\mathrm{H_2}} + E^{\mathrm{ZPE}}_{\mathrm{BDT}} - F^{\mathbf{SU}/\mathrm{Au}}_{\mathrm{vib}}\right)\right] + \gamma_{\mathrm{clean}} - \frac{N_{\mathbf{SU}}}{A}\Delta\mu_{\mathrm{BDT}} \tag{15}$$

The analysis of $\gamma_{\mathbf{LD}}$ ($\Delta\mu_{\mathrm{BDT}}$) together with $\gamma_{\mathbf{SU}}$ ($\Delta\mu_{\mathrm{BDT}}$) provides a clean and unbiased way to compare the relative stability of the different butanedithiol/Au(111) surface structures

3. Results and Discussion

Table 1 shows the average binding energies (E_{b}) estimated by DFT calculations, and the corrected average binding energies ($E_{\mathrm{b}}{}^{\mathrm{c}}$) including the dispersive forces for the BDT phases on the unreconstructed and reconstructed Au(111) surfaces. As expected, the $E_{\mathrm{b}}{}^{\mathrm{c}}$ value per molecule is larger for BDT in the **LD** than the **SU** phase, because each BDT molecule in the **LD** phase has two thiolate-Au bonds while in the **SU** phase it has only one. Also, the **LD** phase includes chain−substrate interactions absent in the **SU** phase. Nevertheless, the binding energy for the **LD** phase is not twice that estimated for **SU**, because the configuration of the BDT molecule in the **LD** phase seems to be less favored than that reached in the **SU** phase. Note also that the **LD** phase has half the number of molecules in the unit cell as the **SU** phase.

(30) *JANAF Thermochemical Tables*, 2nd ed., U.S. National Bureau of Standards, Washington, DC, 1971

(31) Lavrich D. J.; Cummings T.; Bernasek S. L.; Scoles G. *J. Phys. Chem. B* **1998**, *102* (46), 9266−9275

(32) Vericat, C.; Vela, M. E.; Salvarezza, R. C. *Phys. Chem. Chem. Phys.* **2005**, *7*, 3258–3268.

Table 1. Binding Energies for the LD and SU BDT Phases on the U and R Au(111) Substrates[a]

Au(111) surface	adsorbate phase	E_b/eV	E_b^c/eV
unreconstructed (U)	**LD**	−3.30	−3.56
	$\mathbf{SU}_{\sqrt{3}\times\sqrt{3}\ R30^\circ}$	−1.80	−1.98
	$\mathbf{SU}_{C4\times2}$	−1.79	−1.97
reconstructed (R)	**LD**	−4.28	−4.54
	$\mathbf{SU}_{C4\times2}$	−2.25	−2.43

[a] E_b is average adsorption energy of BDT with respect to the corresponding clean surface and the adsorbate energies, E_b^c is the corrected E_b after including dispersive forces (E_{vdW}) as indicated in the text.

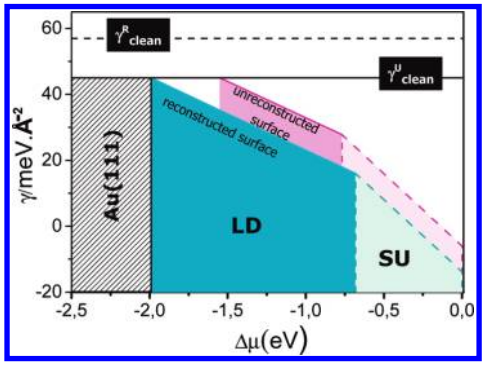

Figure 3. $\gamma_{\mathbf{LD}}$ and $\gamma_{\mathbf{SU}}$ vs $\Delta\mu$ for BDT phases on the U (pink) and R (blue) Au(111) surfaces. $p_{H_2} = 10^{-10}$ atm. The γ_{clean} values for U and R surfaces are also indicated.

Results in Table 1 show that for a given BDT phase E_b^c is larger on the R than that on the U surface.[16,33] There are important differences in the E_b^c values (ΔE_b^c) for **LD** and **SU** phases on the U and R substrates: $\Delta E_b^c = E_b^c(\mathbf{LD}_R) - E_b^c(\mathbf{LD}_U) = -0.98$ eV and $\Delta E_b^c = E_b^c(\mathbf{SU}_R) - E_b^c(\mathbf{SU}_U) = -0.45$ eV, respectively. Thus, the presence of Au adatoms at the surface has a greater influence in the binding energy for the **LD** phase than for the **SU** phase.

Figure 3 shows the surface free energy for the different BDT phases on the U and R substrates as a function of the chemical potential of the adsorbate calculated with eqs 14 ($\gamma_{\mathbf{LD}}$) and 15 ($\gamma_{\mathbf{SU}}$) for $p_{H_2} = 10^{-10}$ atm. The surface free energies of the clean U ($\gamma^U{}_{clean}$) and the clean R surface ($\gamma^R{}_{clean}$) estimated by eq 13 are also included. As expected, the surface free energies of the clean substrate surfaces are independent of the chemical potential of the BDT molecules; thus, they appear as lines parallel to the x-axis. The free energy of the clean R cell is larger than that of the U surface, because it involves the energy cost to form the Au adatoms. On the other hand, the different BDT phases on both U and R surfaces yield γ vs $\Delta\mu$ straight lines whose slope is determined by the N_X/A ratio where X stands for **LD** or **SU** (note that A is constant for all surface structures). At low chemical potentials ($\Delta\mu \rightarrow -\infty$), the BDT surface structures exhibit surface free energy values more positive than the $\gamma^U{}_{clean}$, reflecting that they are unstable with respect to the clean surface. However, when $\Delta\mu = -2.0$ eV for the R substrate and $\Delta\mu = -1.55$ eV for the U substrates the **LD** phases become more stable than the clean surface. The chemical potential range for the thermodynamic stability of the **LD** phases extends up to $\Delta\mu = -0.68$ eV for BDT on R and −0.77 eV for BDT on U where the intersections between the $\gamma_{\mathbf{LD}}$ and $\gamma_{\mathbf{SU}}$ lines is observed indicating a phase transition (Figure 3).

The increase in p_{H_2} from 10^{-10} atm to 5×10^{-7} atm results in an increase in the stability range of the clean surface, i.e., BDT adsorption to form the **LD** is more difficult. In fact, the clean surface is now covered by the **LD** phase only when $\Delta\mu = -1.77$ eV for the R and $\Delta\mu = -1.32$ eV for U surfaces. In contrast, the **LD** to **SU** phase change takes place also at $\Delta\mu = -0.68$ eV and −0.77 eV for BDT on R and U surfaces indicating that the phase transition is not influenced by the p_{H_2} value. Therefore, the overall effect of increasing the hydrogen pressure is to shorten the stability of the **LD** phase. We can explain the independence of the **LD** to **SU** phase change on p_{H_2} by considering that the formation of the **SU** phase takes place at the expense of the **LD** phase according to the following reaction

$$\mathrm{BDT}_{\mathbf{LD}}/\mathrm{Au}(111) + \mathrm{BDT} \rightarrow 2\mathrm{BDT}_{\mathbf{SU}}/\mathrm{Au}(111) \qquad (16)$$

Figure 3 also shows that the difference in the surface free energy between the **LD** phases on the R and U surfaces is ~10 meV Å^{-2}, while the same difference for the **SU** phases is ~8 meV Å^{-2}. As the error involved in our calculations is ~3 meV Å^{-2} (considering that the error in E_b estimation is less than 0.05 eV, and the cell area), these differences are significant. It means that both **LD** and **SU** phases are more stable on the R surface, i.e., there is a clear driving force to reconstruct the Au(111) surface upon BDT adsorption.

Now, we discuss the **LD** to **SU** phase transition for α,ω-dithiols with longer hydrocarbon length chain. For this purpose, we analyze the adsorption of two α,ω-dithiols, named nDT, hexanedithiol (HDT) and nonanedithiol (NDT) on the U and R surfaces.

Let us consider a rectangular cell $\sqrt{3}\times3$ where only one BDT molecule in the **LD** phase and two BDT molecules in the **SU** phase are chemisorbed. In both cases, there are two S−Au thiolate bonds per unit cell. We start with BDT in the **LD** phase with the molecular plane parallel to the surface and the hydrocarbon backbone extended along the $\langle 1\bar{1}0\rangle$ direction. When an α,ω-alkanedithiol with a higher number of carbon atoms is adsorbed, the y-component of the unit cell ($\sqrt{3}\times3$) increases in a proportional way, and the new unit cell should be ($\sqrt{3}\times3\lambda$) where $\lambda = n_c/4$ is a factor that relates the number of C atoms between the HDT or NDT and the BDT molecules. Thus, the area of the unit cell for longer dithiols can be related to the area of BDT unit cell as $A\cdot\lambda$. In contrast, for the **SU** phase the number of dithiol molecules (and S−Au bonds) remains independent of n_c. Now, we consider the difference in stability related to the change in chain/chain and substrate/chain interactions with n_c. Therefore, eqs 14 and 15 for longer dithiols can be modified as

$$\gamma_{\mathbf{LD}}(\Delta\mu_{nDT}) = \frac{N_{\mathbf{LD}}}{A\lambda}\left[\left(E_b^{\mathrm{LD/Au}} - n_C 0.064\right) - \left(E_{BDT} - E_{\mathbf{LD}} - \mu_{H_2} + E_{nDT}^{ZPE} - F_{vib}^{\mathrm{LD/Au}}\lambda\right)\right] + \gamma_{clean} - \frac{N_{\mathbf{LD}}}{A\lambda}\Delta\mu_{nDT} \qquad (17)$$

$$\gamma_{\mathbf{SU}}(\Delta\mu_{nDT}) = \frac{N_{\mathbf{SU}}}{A}\left[\left(E_b^{\mathrm{SU/Au}} - n_C 0.044\right) - \left(E_{BDT} - E_{\mathbf{SU}} - \frac{1}{2}\mu_{H_2} + E_{nDT}^{ZPE} - F_{vib}^{\mathrm{SU/Au}}\lambda\right)\right] + \gamma_{clean} - \frac{N_{\mathbf{SU}}}{A}\Delta\mu_{nDT} \qquad (18)$$

Note also that the term F_{vib} should be corrected by the λ parameter considering the vibrational contribution to free energy for the adsorbed HDT and NDT species.

(33) Bencini, A.; Rajaraman, G.; Totti, F.; Tusa, M. *Superlat. Microstr.* **2009**, *46*, 4–9.

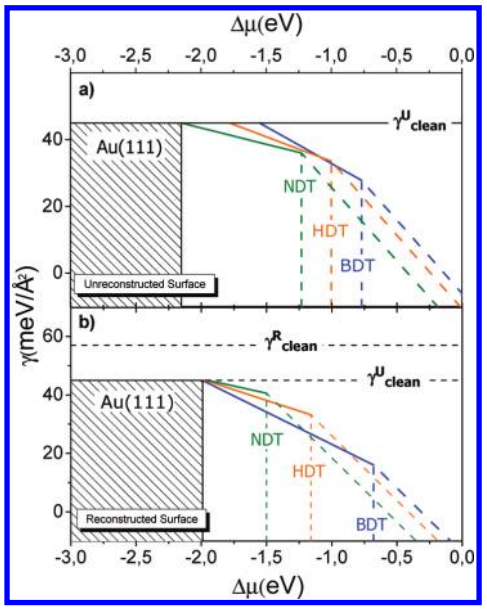

Figure 4. γ_{LD} and γ_{SU} vs $\Delta\mu$ ($p_{H_2} = 10^{-10}$ atm) for BDT (blue), HDT (orange), and NDT (green) adsorbed on (a) unreconstructed and (b) reconstructed Au(111) surfaces. γ_{LD} (solid lines), γ_{SU} (dashed lines). Clean surfaces (black). The transition points are indicated by vertical lines.

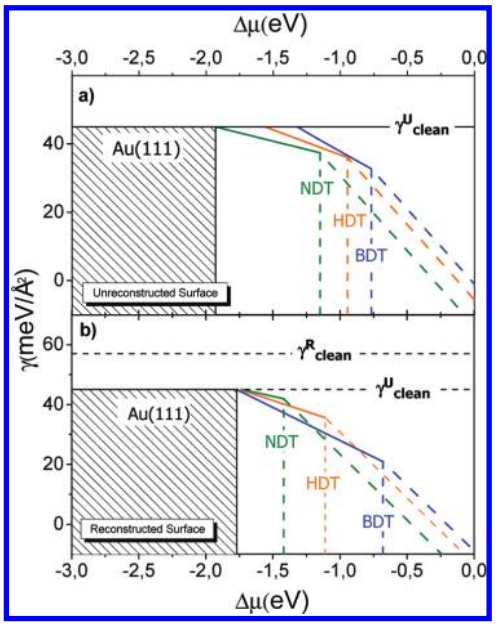

Figure 5. γ_{LD} and γ_{SU} vs $\Delta\mu$ ($p_{H_2} = 5 \times 10^{-7}$ atm) for BDT (blue), HDT (orange), and NDT (green) adsorbed on (a) unreconstructed and (b) reconstructed Au(111) surfaces. γ_{LD} (solid lines),γ_{SU} (dashed lines). Clean surfaces (black). The transition points are indicated by vertical lines.

The phase diagrams for BDT, HDT, and NDT on the U and R surfaces drawn by using eqs 17 and 18 for $p_{H_2} = 10^{-10}$ atm are shown in Figure 4a,b. The diagram in Figure 4a reveals that the formation of **LD** phases on U surfaces takes place at lower $\Delta\mu$ values (they becomes easier) as n_c is increased, while the formation of the **LD** phase on the R substrate is not affected by n_c. In contrast, the **LD** to **SU** phase transitions are clearly favored by the increase in the hydrocarbon chain length irrespective of the substrate. In fact, the **LD** to **SU** phase transitions are observed at $\Delta\mu = -0.77$ eV for BDT, $\Delta\mu = -1.0$ eV for HDT, and $\Delta\mu = -1.23$ eV for NDT on the U surface (Figure 4a), and $\Delta\mu = -0.68$ eV for BDT, $\Delta\mu = -1.16$ eV for HDT, and $\Delta\mu = -1.5$ eV for NDT on the R surface (Figure 4b). The reason for this behavior is that the stability range of the **LD** phase decreases markedly as the number of dithiol molecules (and thiolate bonds per unit area) is reduced as a consequence of the longer hydrocarbon chains. Another interesting point is that the surface free energy difference between the **LD** phases formed on the R and U surfaces decreases with the hydrocarbon chain length. In fact, this difference is ~ -10 meV Å^{-2} for BDT, while for NDT, it is not significant ($\sim$2 meV Å^{-2}). In contrast, the surface free energy difference observed between **SU** phases formed on R and U substrates are independent of n_c (~ -8 meV Å^{-2}).

We can explain this behavior by using the same argument discussed above: In contrast to what occurs in the **SU** phase, the number of molecules per unit area in the **LD** phase is reduced as n_c is increased. Therefore, the binding energy decreases in going from BDT to NDT making the reconstruction of the Au(111) surface more difficult.

Now, we discuss the effect of p_{H_2} on the stability of these phases. We observe that for $p_{H_2} = 5 \times 10^{-7}$ atm (Figure 5) the formation of the **LD** is more difficult than for $p_{H_2} = 1 \times 10^{-10}$ atm (Figure 4) as $\Delta\mu$ values shift positively when the hydrogen pressure is increased. On the other hand, a similar analysis of data shown in Figures 4 and 5 shows that the increase in the p_{H_2} does not affect the BDT **LD** to **SU** phase transition. For HDT and NDT, the **LD** to **SU** phase transition is slightly more favorable at higher p_{H_2} values because of the change of area between both phases ($A\lambda$ to A).

In order to compare the predictions of the phase diagrams with experimental data reported for SAMs of dithiols on Au(111) prepared from gas phase[8] and from solution deposition,[10] we estimate experimental $\Delta\mu$ values by using eq 9. Statistical thermodynamics have been used to obtain $\mu_0[(T, p)]$ values by means of the molecular partition functions for each α,ω-dithiol (see Supporting Information). In the gas phase, the estimated $\mu_0[(T, p)]$ values are -0.99 eV, -1.1 eV, and -1.3 eV for BDT, HDT, and NDT, respectively. Then, by introducing the μ_0 values, $p_{H_2} = 10^{-10}$, $p_{dithiol}$ 10^{-9} atm, and $T = 300$ K[8] in eq 9 $\Delta\mu$ results in -1.5 eV for BDT, -1.6 eV for HDT, and -1.8 eV for NDT. Thus, from Figure 4 one can conclude that under these experimental conditions the adsorption of BDT, HDT, and NDT on both U (Figure 4a) and R (Figure 4b) surfaces results in the formation of **LD** phases. Our predictions are validated by the observation that only **LD** phases have been experimentally observed for HDT adsorption in the gas phase under these experimental conditions.[8]

In the case of dithiol adsorption from hexane solutions, we have substituted in eq 9 the partial pressure by its molar concentration. On the other hand, the $\mu_0[(T, p)]$ values in the liquid phase have been calculated by using thermodynamic data reported for gas and solution phase (see Supporting Information). Results for $\mu_0[(T, p)]$ values are -0.74 eV, -0.86 eV, and -1.05 eV for BDT, HDT, and NDT, respectively. Then, by introducing the μ_0 values, $p_{H_2} = 5 \times 10^{-7}$, dithiol concentration $= 10^{-3}$ M, and $T = 300$ K[8,10] in eq 9, the corresponding $\Delta\mu$ values are -0.92 eV for BDT, -1.04 eV for HDT, and -1.23 eV for NDT. Therefore, for dithiol adsorption on the U substrate (Figure 5a) one can predict the formation of the **LD** phase for BDT, while for HDT and NDT, the corresponding $\Delta\mu$ values are very close of the transition points, in particular, taking into account the rough approximations involved in our calculations. On the other hand, for dithiol adsorption on the R surface (Figure 5b) we found only **LD** phases for BDT and **SU** phases for NDT that agree well with the experimental XPS data reported in ref 10 (**LD** phases for BDT,

LD + **SU** phases for NDT). On the other hand, for HDT the phase transition is located at $\Delta\mu = -1.10$ eV, a value that can also be considered very close to $\Delta\mu = -1.04$ eV estimated for the experimental conditions. The fact that the chemical potential of HDT in solution is close to the transition point could explain why for HDT only **LD** phases are observed in ref 8 and **LD** + **SU** phases are reported in ref 10. Note, however, that the adsorption mechanism in solution could be more complex[34] so that the comparison between diagram predictions and experimental results is more speculative than that for gas-phase self-assembly.

Finally, it should be noted that the presence of mixed phases in adsorbed HDT and NDT[10] indicates that the phase transition involves a slow kinetics. Hydrogen exchange between the arriving dithiol molecules and the adsorbed thiolates involved in the lying-down phase has been recently proposed as a possible mechanism for this process.[10] This interesting point deserves further theoretical and experimental work.

4. Conclusions

We have presented a comparative study on the thermodynamic stability of the **LD** and **SU** phases of BDT on unreconstructed (U) and on reconstructed (R) Au(111) surfaces. Our DFT calculations show first the coverage of the clean Au(111) surface by the **LD** phase, followed by the **LD** to **SU** phase transition as the chemical potential of the BDT molecule is increased. Results from these calculations show that the **LD** and **SU** phases are more stable on the R than on the U Au(111) surfaces, suggesting that the Au(111) surface should reconstruct upon BDT adsorption. We extend our analysis to longer α,ω-dithiols. The analysis reveals that the **LD** to **SU** phase transition is favored as the hydrocarbon chain length of the dithiol molecules is increased. Changes in the hydrogen pressure affect the formation of the **LD** phase, while they have no significant effects on the **LD** to **SU** phase transition. The parameters that control the thermodynamic stability of the different phases are the binding energy of the adsorbates and the number of adsorbed species per unit of substrate area.

Our calculations explain the influence of the number of carbon atoms in the hydrocarbon chains, hydrogen pressure, and dithiol pressure (or concentration) on dithiol adsorption and phase transitions. This information is relevant to control the coverage, reactivity, and surface chemistry of the dithiol self-assembled monolayers on Au(111) surfaces.

Acknowledgment. We acknowledge financial support from ANPCyT (Argentina, PICT06-621) and CONICET (Argentina, PIP 112-200801-362) and MCI (Spain, CTQ2008-06017/BQU). A.M. acknowledge financial support from Spanish MCIIN MAT2007-65990-C03-03 and CSD2007-00045.

Supporting Information Available: The calculations of the zero point energies (E_{nDT}^{ZPE}), vibrational contributions to the Gibbs free energy for the adsorbed system (F_{vib}), $\mu_{nDT}^{0}(T, p^{0})$, and $\mu_{nDT}^{0}(T, p^{0})_{LIQ}$ are available. Also, the DFT electronic energies of BDT, LD, SU, and H_2 are presented. This material is available free of charge via the Internet at http://pubs.acs.org.

(34) Hasan, M.; Bethell, D.; Brust, M. *J. Am. Chem. Soc.* **2002**, *124*, 1132–1133.